

Original

Received August 31, 2001  
 Accepted for Publication December 17, 2001  
 ©2000 Soc. Mater. Eng. Resour. Japan

## Iron Matrix Transformations and Mechanical Properties of Fe-25Cr-C-B Eutectic Cast Alloys

Widia HARTONO\*, Setsuo ASO\*\*, Shoji GOTO\*\* and Yoshinari KOMATSU\*\*

\*Graduate School of Mining and Engineering, Akita University, 1-1,  
 Tegata-Gakuen-Cho, Akita, 010-8502 Japan  
*E-mail : widh@ipc.akita-u.ac.jp*

\*\*Department of Material Engineering, Faculty of Engineering and Resource Science,  
 Akita University, 1-1, Tegata-Gakuen-Cho, Akita, 010-8502 Japan

Iron matrix transformation behavior and high temperature strength of Fe-25mass%Cr-C-B cast alloys were investigated using thermal expansion method and compressive test, respectively. Five kinds of eutectic alloys were destabilized at temperatures of 1173 K, 1273 K and 1373 K for 1800 and 18000 seconds, followed with air cooling. Compressive test was made on Fe-25Cr-0C-2.2B, Fe-25Cr-2.2C-1.0B and Fe-25Cr-3.5C-0B eutectic alloys at temperatures up to 1073 K. Result of the work shows that  $M_s$  temperature rises with the decrease in destabilization temperature, but the hardness becomes larger with the increase in destabilization temperatures, for the alloys with boron content. Compressive strength of all as-cast alloys was above 2000 MPa at room temperature and above 100 MPa even at 1073 K. The true stress-true strain curves characteristics depended on the chemical composition of the alloys. The effect of destabilization heat treatment almost disappears at the temperatures above 873 K in every alloys.

**Key Words** : high chromium white cast iron, iron matrix transformation, compressive strength.

### 1. Introduction

High chromium white cast irons are used in a variety of applications where stability in an aggressive environment is a principal requirement, including the mining and mineral processing, cement production, and pulp and paper manufacturing industries. Superior abrasive wear resistant, combined with relatively low production costs, make these alloys particularly attractive for applications where grinding, milling and pumping apparatuses are used to process hard materials such as ore, coal, gravel and cement<sup>[1]</sup>.

With the advent of a 25 to 30mass%Cr, this high chromium white cast iron was significantly more wear resistant than unalloyed white cast iron. The microstructures of white cast irons can be described as heterogeneous mixtures of randomly-oriented bundles of carbides with morphologies of plates, laths or rods embedded in a matrix of austenite ( $\gamma$  Fe), martensite, pearlite, bainite and/or ferrite ( $\alpha$  Fe)<sup>[2]</sup>. The excellent resistant to abrasion, corrosion and oxidation of high chromium white cast irons not only depend on eutectic carbide, but also are strongly affected by matrix structure.

In order to improve the properties of the high chromium cast irons, the addition of various chemical compositions was studied. With boron addition to the high chromium white cast irons, most of boron is solidified to boride and/or borocarbide, in the Fe-25mass%Cr-C-B system alloys.

Due to the high carbon and alloy content of the high chromium white cast irons, the metastable austenite is often retained in the

as-cast structure. Hence, the microstructure formed in as-cast condition is a matrix of austenite, which may partially transform to martensite, bainite and pearlite. Although it is the carbides which most strongly determine the abrasion resistance, it is often desirable to harden this matrix structure through the use of heat treatment. The aim of most heat treatments is to convert the austenite matrix to the harder martensite phase.

In this research, to clarify the iron matrix transformation behavior of Fe-25mass%Cr-C-B cast alloys, five kinds eutectic alloys with different carbon and boron contents were destabilized at temperatures of 1173 K, 1273 K and 1373 K for 1800 s and 18000 s under argon atmosphere using thermal expansion method. In addition, compressive test was made on Fe-25Cr-0C-2.2B, Fe-25Cr-2.2C-1.0B and Fe-25Cr-3.5C-0B eutectic alloys at temperatures up to 1073 K to investigate the high temperature strength characteristics of the alloys.

### 2. EXPERIMENTAL PROCEDURE

The specimens used in this study were 6 kinds of eutectic alloys lying on the eutectic lines of liquidus surface phase diagram Fe-25Cr-C-B system, as shown in Fig. 1. The specimens were melted in a high frequency induction furnace with argon gas atmosphere and poured into sand mold (produced using CO<sub>2</sub> process), in which 20 pieces of silica tubes were inserted to make cylindrical shape specimens. The chemical composition of the specimens was investigated by EDS and listed in Table 1.

Destabilization heat treatment was attempted using thermal

expansion test method. The cylindrical specimen with the size  $\phi$  8 mm  $\times$  40 mm was inserted into dilatometer, heated to 1173 K, 1273 K and 1373 K of the destabilization temperatures for 1800 s and 18000 s respectively, and subsequently cooled with cooling rate of 3 K/s. The result was recorded to thermal expansion graphs.

High temperature compressive test equipment used for compressive test was set into Shimadzu's Universal Testing Machine. As-cast and destabilized (1273 K, 1800 s) specimens were cut into  $\phi$  4.5 mm  $\times$  10 mm cylindrical shape. The test conditions were as follows. Test temperatures were room temperature (RT), 473, 573, 673, 773, 873, 973 and 1073 K, with the initial strain rates of  $2.5 \times 10^{-4}$ ,  $8.3 \times 10^{-4}$ ,  $2.5 \times 10^{-3}$  and  $1.7 \times 10^{-2} s^{-1}$ . Because of maximum compressive stress in the temperature below 673 K was

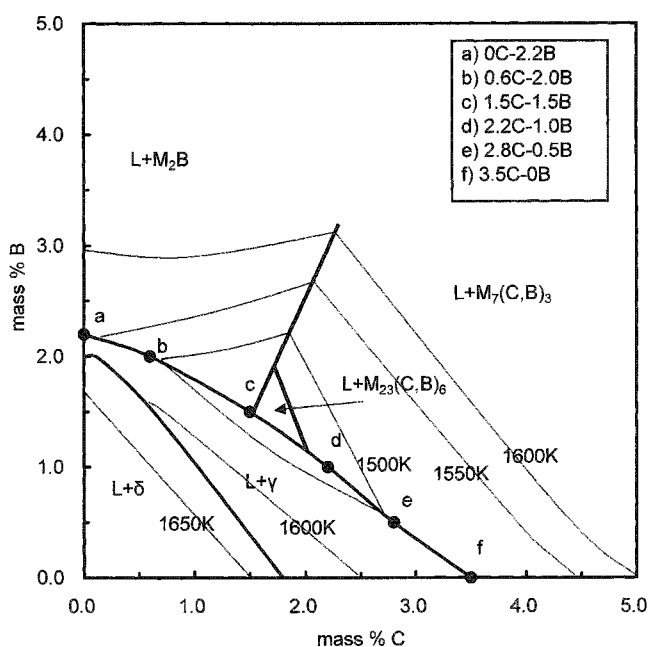


Figure 1 Liquidus surface phase diagram of the Fe-25%Cr-C-B system.

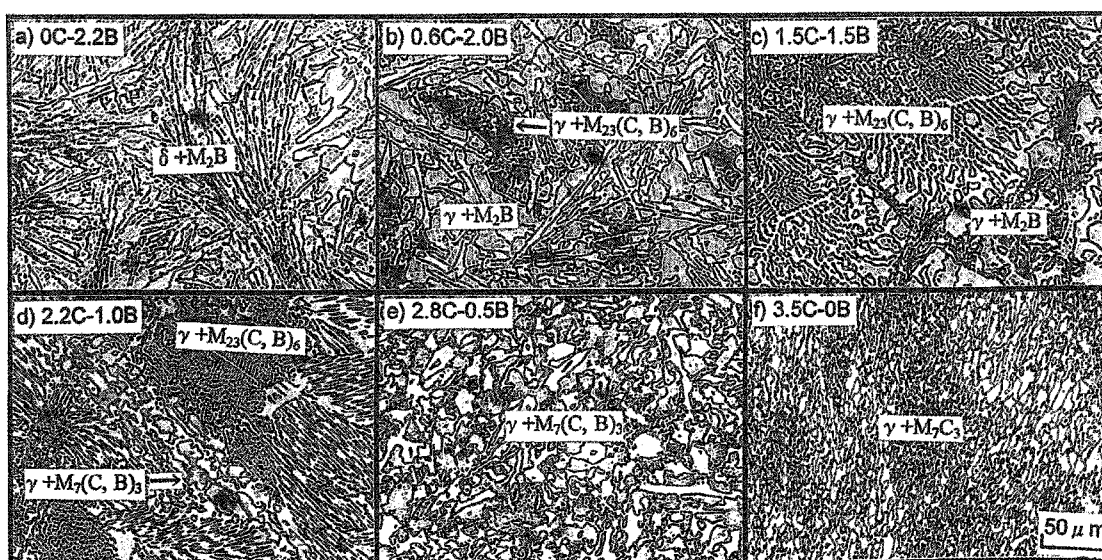


Figure 2 Microstructure of as-cast specimens.

Table 1 Chemical composition of the specimens.

| (a) Destabilization heat treatment |                              |      |      |      |
|------------------------------------|------------------------------|------|------|------|
| Alloy                              | Chemical composition (mass%) |      |      |      |
|                                    | Cr                           | C    | B    | Fe   |
| b) 0.6C-2.0B                       | 25.39                        | 0.58 | 1.76 | bal. |
| c) 1.5C-1.5B                       | 24.87                        | 1.57 | 1.45 | bal. |
| d) 2.2C-1.0B                       | 29.94                        | 2.45 | 1.00 | bal. |
| e) 2.8C-0.5B                       | 26.12                        | 2.88 | 0.71 | bal. |
| f) 3.5C-0B                         | 24.66                        | 3.11 | 0.00 | bal. |
| (b) Compressive test               |                              |      |      |      |
| Alloy                              | Chemical composition (mass%) |      |      |      |
|                                    | Cr                           | C    | B    | Fe   |
| a) 0C-2.2B                         | 25.63                        | 0.30 | 2.39 | bal. |
| d) 2.2C-1.0B                       | 25.69                        | 1.98 | 1.18 | bal. |
| f) 3.5C-0B                         | 27.54                        | 3.52 | 0.00 | bal. |

little affected by changing strain rate, only the strain rate of  $2.5 \times 10^{-4} s^{-1}$  was used in these temperatures. To prevent the oxidation to the specimens the test was done in the argon gas atmosphere.

Solidification structure of the specimens was verified by optical microscopy. The scanning electron microscopy was used to characterize the matrix transformation before and after destabilization and the microstructures after compressive test.

### 3. RESULTS

#### 3.1 Solidification structure

Figure 2 shows the solidification structure of the specimens. As shown in Fig. 1, with the increase of carbon content and the decrease of boron content of the alloys, the microstructure was changing from  $\delta + M_2B$  eutectic structure (0C-2.2B alloy) to  $\gamma + M_2B$  and  $\gamma + M_{23}(C, B)_6$  eutectic structures (0.6C-2.0B and 1.5C-1.5B alloys). In the high C (low B) side, the microstructures of  $\gamma + M_{23}(C, B)_6$  and  $\gamma + M_7(C, B)_3$  in 2.2C-1.0B alloy were changing to  $\gamma + M_7(C, B)_3$  in 2.8C-0.5B alloy and finally to commonly  $\gamma + M_7C_3$  structure in the 3.5C-0B alloy. Even the

eutectic structures of 0.6C-2.0B and 1.5C-1.5B alloys are consist of  $\gamma + M_2B$  and  $\gamma + M_{23}(C, B)_6$ , the eutectic structure of these alloys is not similar, due to the difference in order of crystallization.

The iron matrices of the alloys shown in Fig. 2 are the mixture of ferrite and bainite for 0C-2.2B alloy, retained austenite, bainite and martensite for 0.6C-2.0B, 1.5C-1.5B, 2.2C-1.0B and 2.8C-

0.5B alloys and the mixture of pearlite and retained austenite for 3.5C-0B alloys, respectively.

### 3.2 Destabilization Heat Treatment

The aim of destabilization heat treatment is to destabilize the austenite matrix, thereby promoting transformation of the

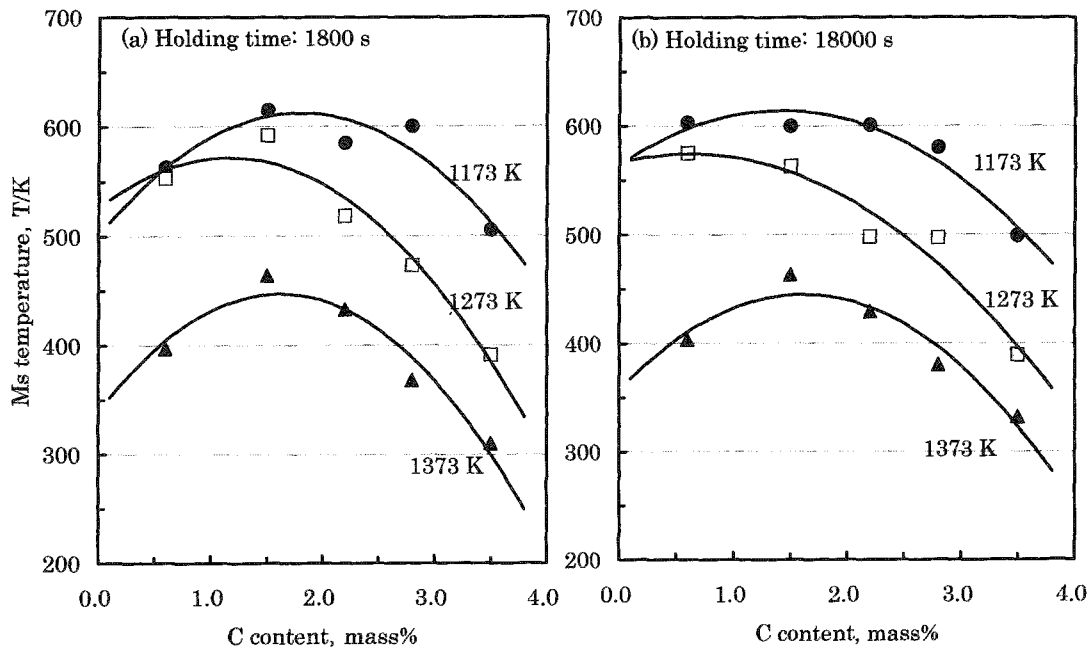


Figure 3 Relationship between Ms temperature and destabilization conditions.

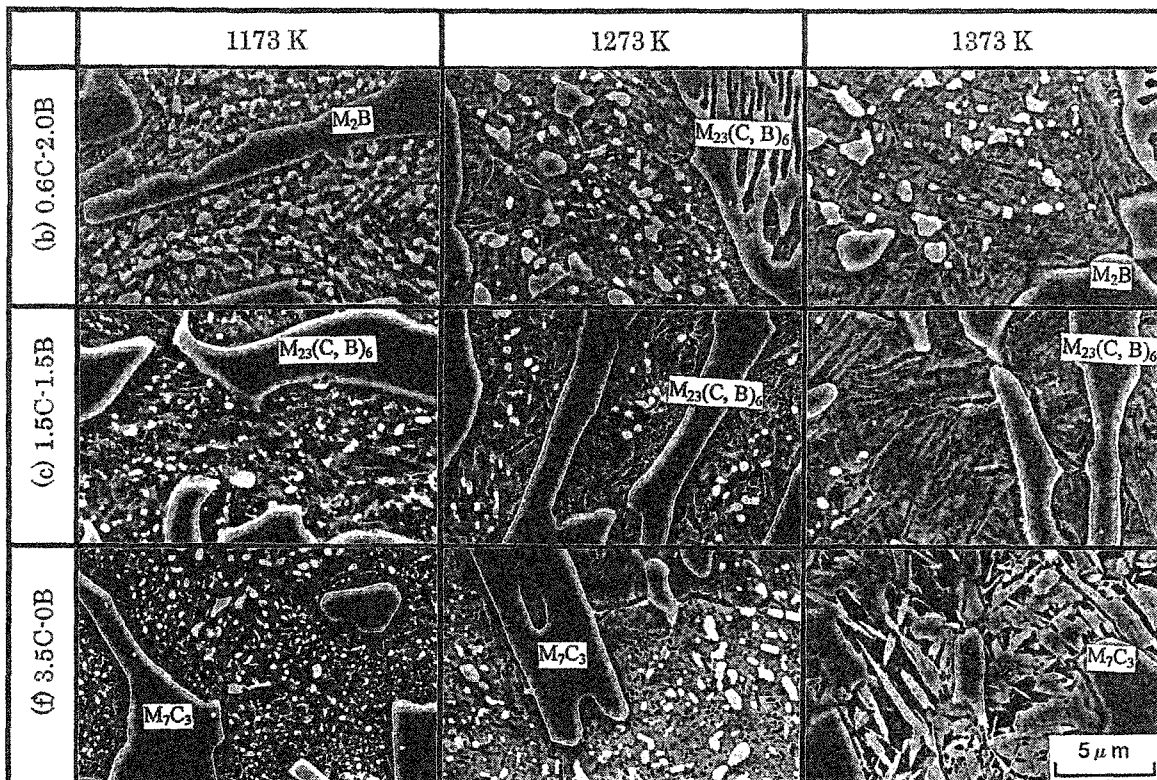


Figure 4 SEM photographs of the alloys after destabilization for 18000 s.

austenite to martensite. While at this elevated temperature (and during the heat-up to and cooling from), secondary carbides precipitate within the austenite matrix. As these carbides form, they deplete the surrounding austenite of alloying elements, thereby destabilizing it. The lower alloy content of destabilized austenite increases the martensite start ( $M_s$ ) temperature. Air cooling following the destabilization heat treatment is usually sufficient to produce transformation of the austenite to martensite.

The relationship between  $M_s$  temperature obtained from thermal expansion graphs and carbon content of the 5 kinds alloys is shown in Fig. 3. For both of the holding times, the raise of destabilization temperature lowers  $M_s$  temperature. Except of 0.6C-2.0B alloys, which have the lowest carbon content, for the other alloys the increase of carbon content lowers  $M_s$  temperature, which is similar with the heat treatment of steel materials. However,  $M_s$  temperature is little affected by changing holding time from 1800 s to 18000 s, as shown in Fig. 3.

Figure 4 shows SEM photographs of the transformed matrix structure of 0.6C-2.0B, 1.5C-1.5B and 3.5C-0B after destabilized for 18000 s in various destabilization temperatures. In as-cast condition, matrix structures of the alloys were the mixtures of retained austenite and bainite for both 0.6C-2.0B and 1.5C-1.5B alloys, where retained austenite and pearlite are shown in 3.5C-0B alloy. After destabilization, iron matrix transformed to martensite for all destabilization conditions, the amount of secondary carbides decreases with the increase of destabilization temperature. However, there is a large amount of retained austenite beside of martensite in the 3.5C-0B alloy after destabilized in 1373 K.

The micro-hardness of the matrix depends on the transformation behavior of matrix microstructure, which is related to the alloy content of the matrix. In the case of destabilization heat treatment, destabilization temperature, holding time and the cooling rate after destabilization influence the final matrix structures of the alloys. Figure 5 shows the matrix hardness of the destabilized

alloys. In as-cast condition, 0.6C-2.0B, 1.5C-1.5B and 2.2C-1.0B alloys show the higher hardness due to the presence of bainite in the matrix structure beside of retained austenite.

Although almost the matrix structure consist of retained austenite, as-cast 2.8C-0.5B alloy shows the hardness of Hv770, because of the high content of carbon in the solid solution of the matrix. However, all of the alloys show the hardness above Hv600 after the destabilization heat treatment. Except of 3.5C-0B alloy the rise of destabilization temperature increases the hardness of the matrix for both the holding times. For the similar cooling rate, the solubility of the alloy content, such as carbon and chromium in the austenite increases with the increase of the destabilization temperature, so that the martensite obtained after cooling becomes harder.

The hardness of 3.5C-0B alloy, on the other hand, remarkably decreased at the 1373 K, since the rise of destabilization temperature decreases  $M_s$  temperature, thereby reduces the amount of martensite obtained after cooling and increases the lower hardness austenite<sup>[3]</sup>. However, the hardness is almost not affected by the change of holding time.

### 3.3 Results of Compressive Test

Figure 6 shows true stress-true strain curves of the as cast and destabilized (1273 K, 1800 s) conditions of 0C-2.2B, 2.2C-1.0B, and 3.5C-0B alloys. Initial strain rate used in Fig. 6 is  $2.5 \times 10^{-4} \text{ s}^{-1}$ . Ultimate compressive stress ( $\sigma_b$ ) of all of the alloys decreases with the rise of test temperature. The characteristic of true stress-true strain curves of the alloys depends on chemical composition of the alloys.

In the as-cast condition, 0C-2.2B alloy fractured immediately after the elastic limit at the room temperature, but showed the plastic deformation with work hardening, in which the strain amount to ultimate compressive stress is nearly maximum strain, at the temperature range from 473 K to 773 K. At the tempera-

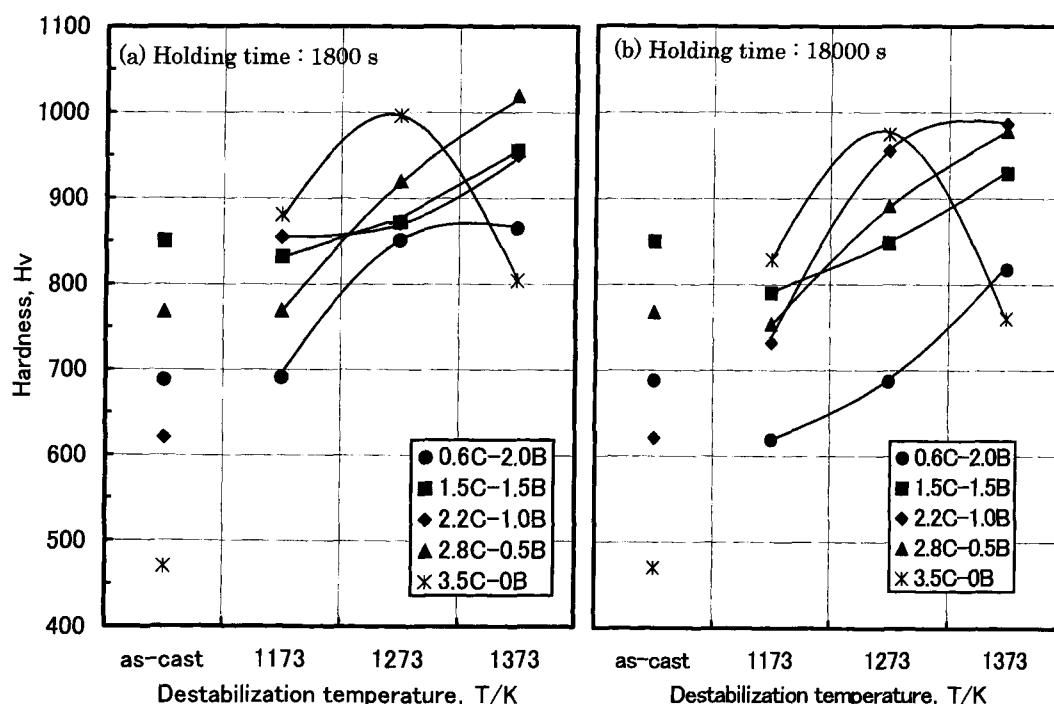


Figure 5 Matrix hardness of the alloys.

tures above 873 K, the stress is apparently constant after the ultimate compressive stress in the initial deformation. On the contrary, 2.2C-1.0B alloys fractured immediately after elastic limit without show plastic deformation at the temperature up to 873 K. In the other hand, the curves at the temperature above 973 K show the work softening type apparently, in which the stress suddenly fall off after showing the ultimate compressive stress at low strain side. True stress-true strain curves of 3.5C-0B alloys at the temperatures below 673 K show the similar shape with these of 0C-2.2B alloys at the temperature range from 473 K to 673 K, show the work softening type at the 773 K and 873 K, and finally the stress is constant after reaching ultimate compressive stress at the temperature above 973 K.

However, at the temperature below 673 K 0C-2.2B alloy shows the compressive strength above 2000 MPa at the temperature test below 600 K, which is higher than that of the other alloys at the same temperature range. At the temperature above 873 K, 2.2C-1.0B alloys show the higher compressive strength than the other alloys. These characteristics of the alloys mostly depend on the difference structure of carbides or borides and iron matrix of the alloys.

In the other hand, the true stress-true strain curves of destabilized 0C-2.2B show the work hardening types below 773 K, and constant after the ultimate compressive stress above 873 K. The compressive strength of the destabilized alloys below 873 K is remarkably lower than that for the as cast alloys, even the fracture strain is higher. The decrease of the compressive strength of these destabilized alloys due to the transformation that occurred in the

iron matrix during destabilization. The mixtures structure of ferrite and bainite of as cast condition transformed to only ferrite structure in the destabilized alloys, with the secondary carbides precipitation.

## 4. DISCUSSION

### 4.1 The effect of chromium content in the matrix on transformation

As shown in Fig. 3, the decrease of  $M_s$  temperature for all of the alloys with the increase of destabilization temperature, is not only related to the change of chromium content but also carbon content, as known in the many materials such as steel. Generally, in the heat treatment when the holding temperature increases,  $M_s$  temperature lowers with the increase of carbon solubility in the iron matrix<sup>[4]</sup>. In this study, it is difficult to make an accurate analysis of the carbon content of the matrix, since the size of analysis area in the specimens is too small, in addition to effect of contamination during analysis. For this reason, the change of chromium concentration in the iron matrix of as cast alloys and destabilized alloys (holding time 18000 s), was analyzed using EDS, and the result is shown in Fig. 7. Chromium concentration of the destabilized alloys is lower than that in the as cast condition, but this concentration increases with the increase of destabilization temperature. With the increase of destabilization temperature, the solubility of carbon and chromium in the austenite also increases, that is why the amount of secondary carbides decreases, as shown in Fig. 4.

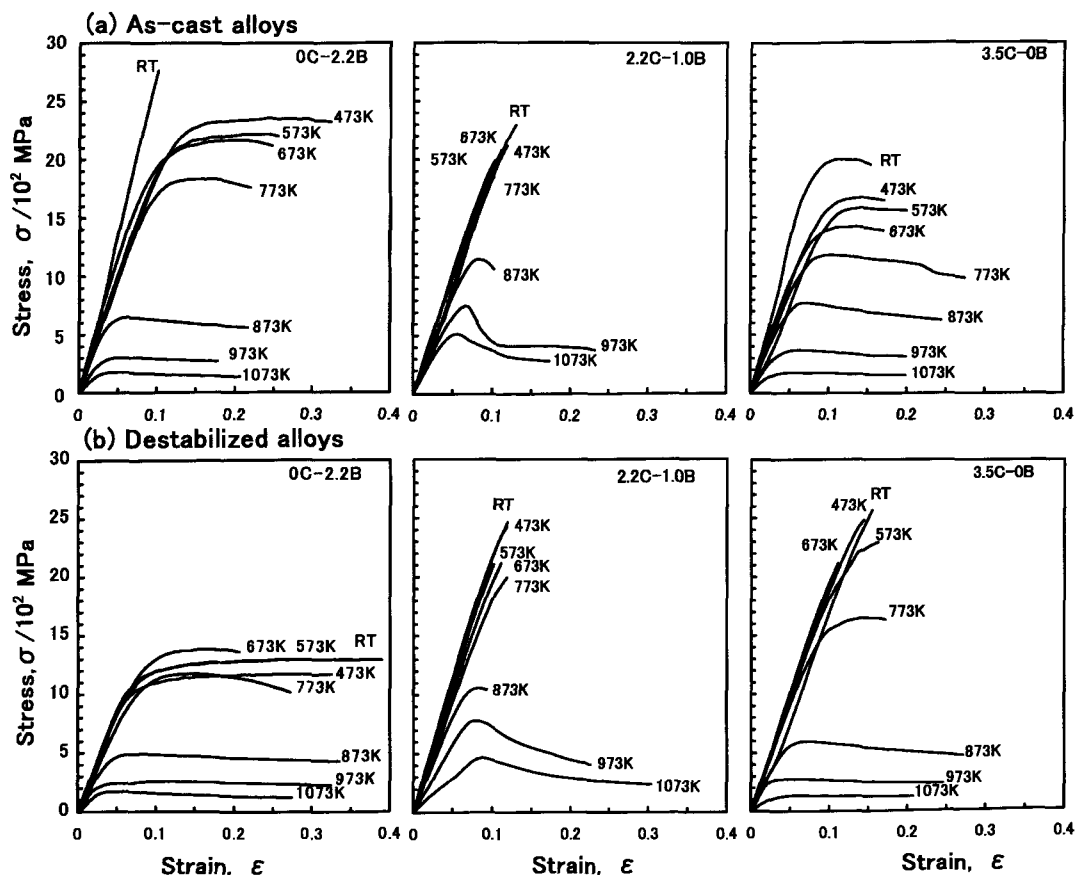


Figure 6 True stress-true strain curves of the alloys tested at a strain rate of  $2.5 \times 10^{-4} \text{ s}^{-1}$ .

#### 4.2 Optimum hardening temperature of the alloys

An optimum destabilization temperature for maximum hardness often exists for high chromium cast irons. This optimum temperature arises from two competing effects, perhaps best illustrated with the aid of Fig. 8<sup>[3]</sup>. In this study, the optimum hardening temperature of 3.5C-0B alloy appeared to be 1273 K for both of the holding times, as shown in Fig. 5. This alloy shows the Ms temperatures below 400 K for both of the holding times, that indicate the high content of retained austenite in the iron matrix. Increased retained austenite lowers the hardness. However, the carbon content of the martensite formed at 1273 K was higher than that of

1173 K, with the decrease of precipitated secondary carbides in the iron matrix, as shown in Fig. 4, and therefore the maximum hardness was obtained.

In the other hand, the hardness of the other alloys increased with the increase of destabilization temperature. It is presumed

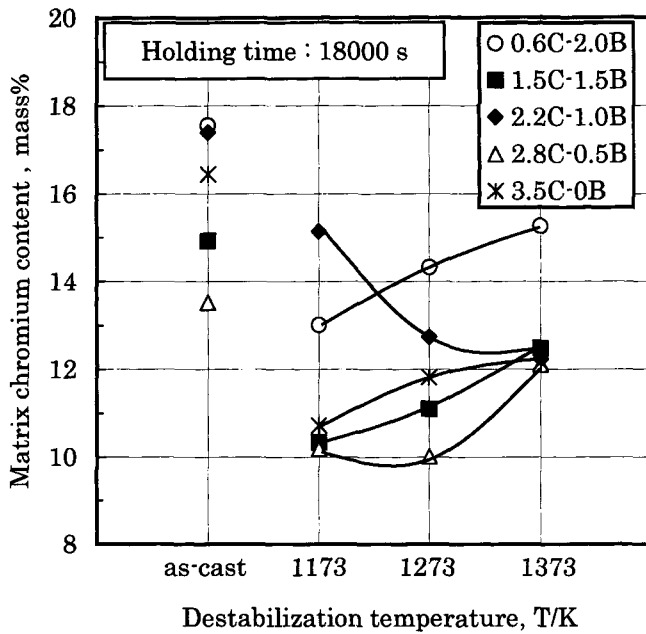


Figure 7 Chromium content of the iron matrix.

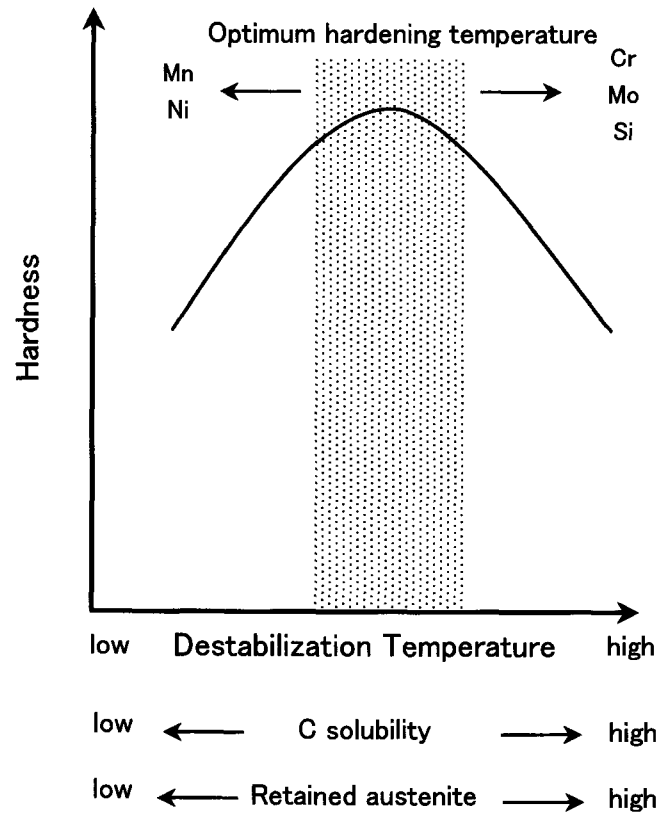


Figure 8 Competing effects in the hardening of high-chromium white irons<sup>[3]</sup>.

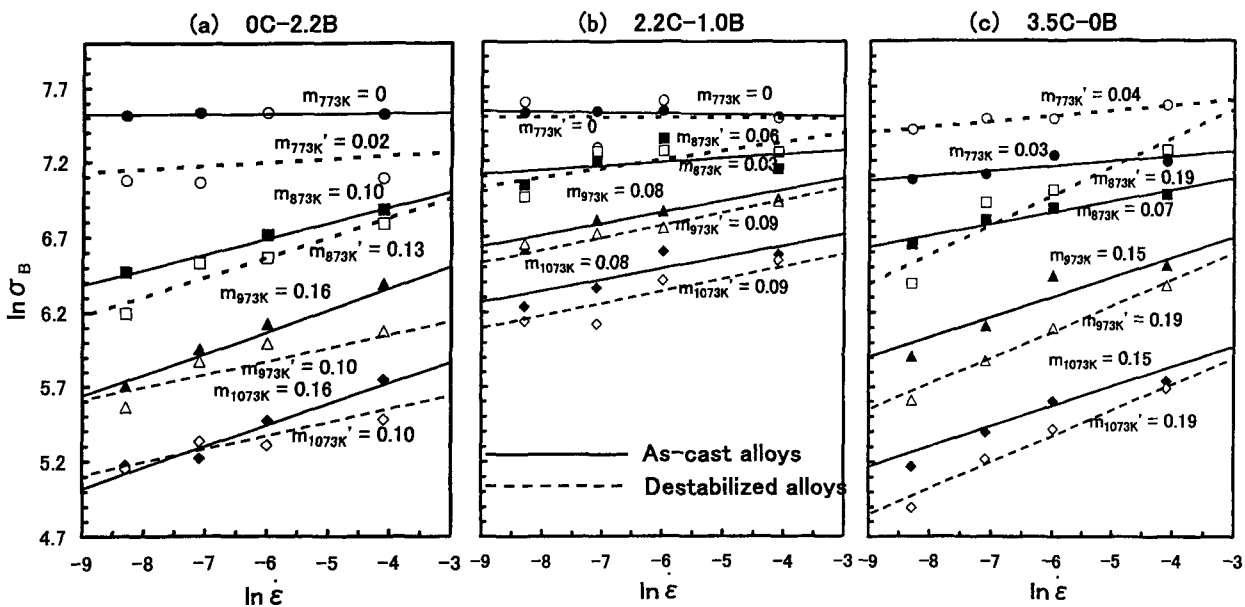


Figure 9 Strain rate dependence of ultimate compressive stress of the alloys.

that the optimum hardening temperature of the alloys was higher than 1373 K, since the increase of chromium content for a given carbon content increases the optimum hardening temperature<sup>[5]</sup>.

#### 4.3 Strengthening mechanism of the alloys

From the results of this study, it is clear that these alloys system have high compressive strength, even at high temperatures. Here, we tried to investigate the strengthening mechanism of the alloys.

Strain rate sensitivity index ( $m$ ) obtained from the logarithmic scales of ultimate compressive stress and strain rate indicates degree of the recovery (decrease of dislocation density) affected by strain rate. The conclusion whether matrix deformation or carbides deformation take a role in the strain rate dependence of  $\sigma_B$  during the compressive test can be predicted by  $m$  measurements. The results of the strain rate dependence of  $\sigma_B$  of the alloys are shown in Fig. 9. It shows that  $m \approx 0$  at 773 K for all the alloys, because at the temperature below  $T_m/2$  ( $T_m$ : melting point) recovery is not occurred, so that strain rate dependence of the strength is not appeared. However,  $m$  increases with the temperatures increase, because the kinetics of the dislocation increases at higher temperatures, while  $\sigma_B$  decreases at the lower strain rate since recovery have enough time to be occurred.

The average of  $m$  value at the temperatures above 873 K of the 0C-2.2B and the 3.5C-0B alloys shown in Fig. 9 are 0.13 and 0.16, respectively. For these alloys, showing that recovery increases at the lower strain rates, it is presumed that the high temperature deformation mostly carried out by the iron matrices. In the other hand, the average of  $m$  value of the 2.2C-1.0B alloy at the temperature above 873 K is 0.07, which is lower than that in the two other alloys. This means the possibility that the dislocation motion did not occur in the  $M_{23}(C, B)_6$  during deformation, or that the recovery did not occur even at the temperature up to 1073 K. Hence, this low  $m$  value indicates that deformation at the 2.2C-1.0B alloy was carried out by deformation of  $M_{23}(C, B)_6$  phase.

Finally, when the iron matrix carry out the deformation of the alloy, the effects of heat treatment will remarkably appear at the lower temperature, but at the higher temperature it depends more on the solidification morphologies of the eutectic alloys than on the iron matrix.

## 5. CONCLUSIONS

- (1) Ms temperature decreases with the increase of destabilization temperature. For the certain destabilization temperature, Ms temperature decreases with the increase of carbon content of the alloys.
- (2) The hardness of the iron matrix is higher with the increase of destabilization temperature. The 3.5C-0B alloys show maximum hardness at 1273 K, the hardness lower at 1373 K.
- (3) Chromium concentration in the destabilized iron matrix lower than in the as cast condition, but this concentration increases with the increase of destabilization temperature.
- (4) The compressive strength of all the as cast alloys was above 2000 MPa, at room temperature and above 100 MPa even at 1073 K. The destabilized alloys also show good high temperature strength.
- (5) The true stress-true strain curves of the 0C-2.2B and 3.5C-0B alloys show a large amount of plastic deformation, reflecting the iron matrix deformation. On the contrary, the 2.2C-1.0B alloy exhibited fracture immediately after the elastic limit.
- (6) The compressive strength of the 0C-2.2B and 3.5C-0B alloys changed in destabilization heat treatment, due to the iron matrix transformation, but the strength of 2.2C-1.0B alloy was only affected slightly by destabilization heat treatment.

## REFERENCES

- [1] Doğan, Ö.N., Hawk, J.A. and Laird II, G., "Solidification Structure and Abrasion Resistance of High Chromium White Irons," Metallurgical and Materials Transact. A, Vol.28A, pp.1315, (1997).
- [2] Laird II, G., "Microstructures of Ni-Hard I, Ni-Hard IV and High-Cr White Cast Irons," AFS Transact. Vol.55, pp.339, (1991).
- [3] Tabrett, C., "Optimum Hardening Temperature of High-Chromium White Irons," Metal Cast. Surface Finish. May/June, pp.43, (1997).
- [4] Jackson, R.S., J., "The Austenite Liquidus Surface and Constitutional Diagram for the Fe-Cr-C Metastable System," Iron Steel Inst., Vol.208, pp.163 (1970)
- [5] Fairhurst, W. and Rohrig, K., "Abrasion-Resistant High-Chromium White Cast Irons," Found. Trade J., 30, pp.685-689 (1974)